

Supplementary Information

Hyper-Rayleigh Scattering in 2D Redox Exfoliated Semi-metallic ZrTe₂ Transition Metal Dichalcogenide

Manoel L. da Silva-Neto^a, Renato Barbosa-Silva^b, Cid B. de Araújo^{a,b}, Christiano J. S. de Matos^c, Ali M. Jawaid^d, Allyson J. Ritter^d, Richard A Vaia^d and Anderson S. L. Gomes^b

^aGraduate Program in Materials Science, Universidade Federal de Pernambuco, Recife, PE 50670-901 Brazil

^bDepartamento de Física, Universidade Federal de Pernambuco, Recife, PE 50670-901 Brazil

^cMackGraphe, Mackenzie Presbyterian University, São Paulo, SP 01302-907 Brazil.

^dMaterials and Manufacturing Directorate, Air Force Research Laboratories, 45433, Ohio, United States.

Synthesis and morphological characterization

Materials. ZrTe₂ in the 1T phase (space group P $\bar{3}$ m1) was purchased from Materion. Acetonitrile (ACN) was purchased from VWR, distilled under nitrogen and stored under activated molecular sieves to prevent moisture accumulation. Cumene hydroperoxide (technical grade, 80%) and hydroquinone (reagent grade, 99%) were purchased from Sigma Aldrich. Note that ZrTe₂ is oxidatively unstable under ambient conditions due to surface mediated hydrolysis. Therefore, storage, exfoliation of bulk powders and thin-film analysis (XPS, Raman, AFM) were carried out with minimal contact to ambient atmosphere.

Exfoliation of ZrTe₂. ZrTe₂ was exfoliated by in-situ polyoxometalate (POM) assembly via the redox exfoliation process^{1,2}. For completeness, the process is also described here. 10 mmol of ZrTe₂ (3500 mg), 50 mL of acetonitrile, and 500 μ L of cumene hydroperoxide were added to a 100mL round bottom flask and stirred under an inert argon atmosphere (50 $^{\circ}$ C; 24 hrs). To initiate POM assembly, a solution of hydroquinone (1 mmol in 10 mL acetonitrile) was added dropwise to the ZrTe₂ slurry, and allowed to stir for 30 minutes at 40 $^{\circ}$ C. The reaction was subsequently transferred to a shear mixer (IKA USA; Turrax T 10) and allowed to exfoliate for 300 minutes at 10,000 rpm. The slurry was then transferred to a centrifuge tube and all particulates were sedimented at 9,000 rpm (8,500 g) for 30 minutes. The supernatant, containing excess oxidant and reductant was discarded and fresh, anhydrous acetonitrile (50 mL) was added to the pellet. The slurry was briefly mixed via a vorticer, and centrifuged again at 9,000 rpm (8,500 g) for 30 minutes. This process was performed three times to ensure complete removal of excess reagents. The exfoliation of bulk powders proceeded via surface adsorption of charged POMs formed in-situ and exfoliated flakes were stabilized with these charged macroanionic POMs. Solutions stored under anhydrous acetonitrile are stable and do not degrade or oxidize in the time frames utilized in this study.

Monolayer size selection of ZrTe₂. Monolayer selection was performed by previously established protocols³. The cleaned slurry containing bulk and exfoliated ZrTe₂ was centrifuged at 400 rpm for 3 hours. The supernatant containing exfoliated ZrTe₂ was collected and subjected to another round of centrifugation at 500 rpm for 3 hours. The supernatant was collected, and subsequently centrifuged at 700 rpm for 3 hours. A light olive color suspension was pipetted out. The concentration of the dispersion was determined by mass difference of a known volume containing flakes, vacuum removal of solvent (100 $^{\circ}$ C; 200 mTorr) and massing the remaining material. The difference in mass results in the amount of ZrTe₂ dispersed in the volume (c.a. 0.10 mg/mL). Monolayer verification was performed via AFM measurements.

Determination of ZrTe₂ stability: To determine the oxidative stability of ZrTe₂ in the dispersion media, films were drop-casted from a dispersion immediately after exfoliation (c.a. 24 hours after exfoliation) and 2 weeks after exfoliation. Both films were analyzed immediately after film preparation. In both cases, negligible oxidation is observed, indicating dispersion of ZrTe₂ flakes in anhydrous solvents protect the material from oxidative degradation. Thus, to ensure accurate compositional and morphological characterization, all thin film samples were deposited under inert atmosphere (dry N₂) and immediately analysed to minimize decomposition of the ZrTe₂ flakes.

AFM measurements. Atomic force microscopy (AFM), Figure S1B, of ZrTe₂ flakes were measured in non-contact tapping mode on a Dimension Icon (Bruker Corporation). AFM cantilevers with an aluminum reflex

coating were used with a resonant frequency of 240 kHz and a force constant of 40 N/m. Samples were diluted in acetonitrile (approximately 1×10^{-9} M) and were drop casted on Si wafers and allowed to dry under inert, anhydrous conditions. The samples were then annealed at 100 °C under dry N₂ for 1 hour prior to imaging, to ensure complete removal of solvent. The Nanoscope Analysis software (Bruker Corporation) was used to determine the statistical distribution of flake thicknesses and lateral sizes (Figures S1C and S1D). At least 100 individual flakes were analysed. An average lateral size of 118 ± 53 nm and an average height of 1.54 ± 0.91 nm were obtained, with measured heights expected to be higher than the actual flakes due to substrate-flake interactions. As the out-of-plane lattice constant for ZrTe₂ is 0.66 nm^{-1} , the measured thickness is compatible with a monolayer-rich ensemble.

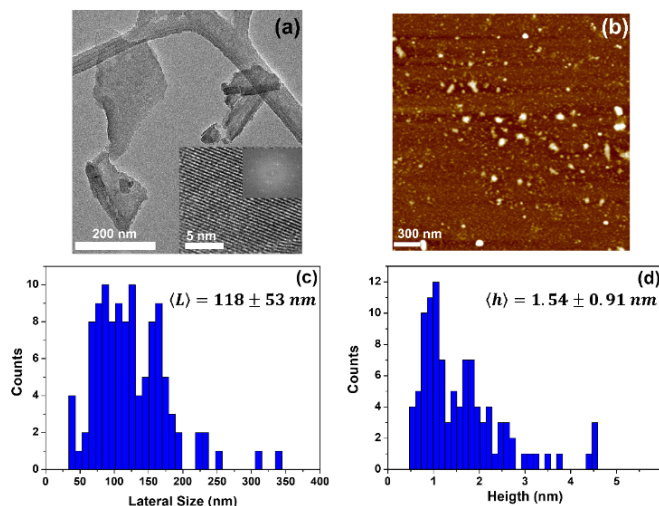


Figure S1. Morphology of exfoliated ZrTe₂ flakes. TEM (A) of monolayer selected ZrTe₂ flakes, scale bar 200 nm. Inset – High resolution image and FFT of basal plane of ZrTe₂ nanoflakes, indicating the single-crystalline morphology is preserved (bar: 5 nm). AFM (B) image of the nanoflakes; lateral size (C) and height (D) distributions of ZrTe₂ flakes. Note, the average height reported via AFM analysis is typically larger than the absolute particle size due to substrate-flake interactions.

Transmission Electron Microscopy. TEM and high resolution TEM (HRTEM) images were collected on an aberration corrected FEI Talos TEM with an accelerating voltage of 200 kV. Samples were prepared by drop-casting colloidal ZrTe₂ dispersions in acetonitrile (10^{-8} M) on lacey-carbon TEM grids. The solvent was wicked off with a kim-wipe after approximately 5 seconds and allowed to dry under dry N₂ (c.a. 1 hour). After drying, samples were immediately transferred to the load-lock chamber to minimize exposure to ambient atmosphere and minimize surface oxidation due to hydrolysis. The morphological results are shown in Figure 1. The inset in Figure S1(A) shows high resolution imaging of the basal surface of ZrTe₂ flakes. The hexagonal packing of the lattice is observed and Fourier transformation of the high-resolution image indicates that single-crystalline ZrTe₂ domains are present.

X-ray Photoelectron Spectroscopy (XPS). ZrTe₂ was drop-casted on silicon wafers and annealed in a thermal oven (1 hr, 100°C) under N₂ to ensure complete solvent removal prior to transfer to the XPS load-lock chamber. X-ray photoelectron spectroscopic analysis was carried out using an SSI XPS System. Survey spectra were acquired using a monochromated Al K α x-ray source (1486.6 eV) operated at 120 W (10 mA, 10 kV) with the electron analyzer operating in hybrid lens mode and an aperture size of approximately 800 μm^2 . Survey data were acquired at an analyzer pass energy of 800 eV, using 1 eV step-sizes and a dwell time of 400 ms. High-resolution data of the Zr 3d, Te 3d, regions were collected using an analyzer pass energy of 30 eV and a step size of 0.1 eV. Data analysis was carried out using the CasaXPS software package. The XPS results are shown in Figures S2S and S2B. The Zr region indicates no surface oxides (ZrO₂ 3d_{5/2} 182 eV) are present on freshly cast films (Fig. S2A). Similarly, the Te 3d region (Fig. S2b) indicates TeO₂ species are not present on the surface (Te 3d_{5/2} TeO₂ = 575 eV). The POM species adsorbed to the ZrTe₂ are not observed due to the percent atomic resolution of the XPS measurements performed.

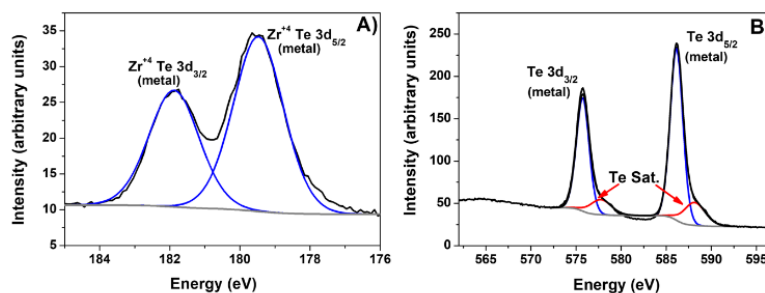


Figure S2. Compositional analysis of ZrTe_2 . XPS spectroscopy of Zr 3d (A) and Te 3d (B) regions indicate the presence of compositional ZrTe_2 .

Raman Spectroscopy. Raman spectra, seen in Figure S3, were collected with a Renishaw inVia confocal Raman microscope. Samples were prepared by drop-casting on Silicon wafers and annealing in a thermal oven at 100°C for 1 hour to ensure complete removal of solvent. After drying, samples were immediately transferred to the analysis chamber and spectra collected to prevent surface hydrolysis. All spectra were collected while under ambient conditions. The excitation laser (at 514.5 nm) was focused onto the few-layered flakes with a 20x objective lens. The power was kept to $100\ \mu\text{W}$ to minimize sample heating. Spectra were collected at acquisition times between 60 – 180 s. The peaks identified in the bulk samples correspond to the E_{2g} (c.a. $116\ \text{cm}^{-1}$) and A_{1g} (c.a. $137\ \text{cm}^{-1}$) modes of the 1T phase⁵. Additional features in the bulk sample corresponding to monoclinic ZrO_2 are observed (indicated by asterisks)⁶. Upon exfoliation, the E_{2g} mode blue-shifts approximately $7\ \text{cm}^{-1}$, as observed for other layered systems^{7,8}, which seems to indicate that no phase change occurred. The absence of ZrO_2 features indicates that the exfoliation process does not lead to significant oxidation of the ZrTe_2 material provided the anhydrous sample preparation.

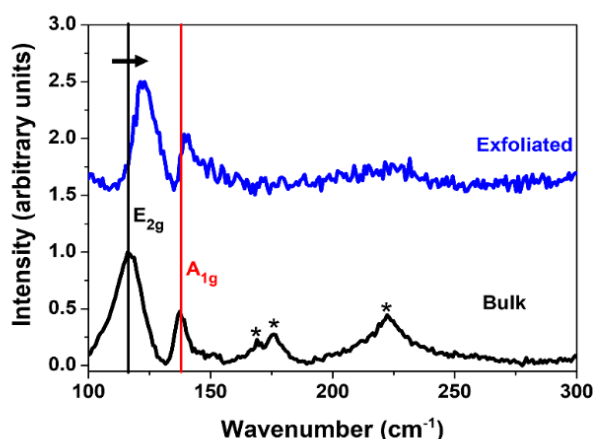


Figure S3 – Raman spectra of ZrTe_2 at 298K (room temperature). Exfoliated and bulk materials are shown for comparison. Observe a blue shift in presumed E_{2g} and A_{1g} modes.

References to Supplementary Information

1. A. Jawaid, J. Che, L. F. Drummy, J. Bultman, A. Waite, M.-S. Hsiao, and R. A. Vaia, *ACS Nano*, **11**, 2017, 635–646.
2. A. M. Jawaid, A. J. Ritter, and R. A. Vaia, *Chemistry of Materials*, 2020, 32, 6550–6565.
3. C. Backes, B. M. Szydłowska, A. Harvey, S. Yuan, V. Vega-Mayoral, B. R. Davies, et. al. *ACS Nano*, **2016**, 10, 1589–1601.
4. I. Kar, J. Chatterjee, L. Harnagea, Y. Kushnirenko, A. V. Fedorov, D. Shrivastava, et.al. *Physical Review B*, **2020**, 101, 165122.
5. M. Hangyo, S.-I. Nakashima, and A. Mitsuishi, *Ferroelectrics*, **1983**, 52, 151–159.
6. D. Eder, and R. Kramer, *Physical Chemistry Chemical Physics*, **2002**, 4, 795–801.
7. H. Li, Q. Zhang, C. C. R. Yap, B. K. Tay, T. H. T. Edwin, A. Olivier, and D. Baillargeat, *Advanced Functional Materials*, **2012**, 22, 1385–1390.
8. F. Wang, I. A. Kinloch, D. Wolverson, R. Tenne, A. Zak, E. O’Connell, et.al. *2D Materials*, **2016**, 4, 015007.